European Heart Journal – Cardiovascular Imaging (2016) **17**, 779–787
doi:10.1093/ehjci/jev206

Endocardial–epicardial distribution of myocardial perfusion reserve assessed by multidetector computed tomography in symptomatic patients without significant coronary artery disease: insights from the CORE320 multicentre study

Jørgen Tobias Kühl[1]*, Richard T. George[2], Vishal C. Mehra[2,3], Jesper J. Linde[1], Marcus Chen[3], Andrew E. Arai[3], Marcelo Di Carli[4], Kakuya Kitagawa[5], Marc Dewey[6], Joao A.C. Lima[2], and Klaus Fuglsang Kofoed[1,7]

[1]Department of Cardiology, Rigshospitalet, University of Copenhagen, 2012, The Heart Centre, Blegdamsvej 9, 2100 Copenhagen, Denmark; [2]Department of Medicine, Johns Hopkins University, Baltimore, MD, USA; [3]National Heart, Lung and Blood Institute, National Institutes of Health, Bethesda, MD, USA; [4]Brigham and Women's Hospital, Boston, MA, USA; [5]Mie University Hospital, Tsu, Japan; [6]Charitè Medical School, Humboldt, Berlin, Germany; and [7]Department of Radiology, Rigshospitalet, University of Copenhagen, Copenhagen, Denmark

Received 18 March 2015; accepted after revision 2 August 2015; online publish-ahead-of-print 4 September 2015

Aim Previous animal studies have demonstrated differences in perfusion and perfusion reserve between the subendocardium and subepicardium. 320-row computed tomography (CT) with sub-millimetre spatial resolution allows for the assessment of transmural differences in myocardial perfusion reserve (MPR) in humans. We aimed to test the hypothesis that MPR in all myocardial layers is determined by age, gender, and cardiovascular risk profile in patients with ischaemic symptoms or equivalent but without obstructive coronary artery disease (CAD).

Methods and results A total of 149 patients enrolled in the CORE320 study with symptoms or signs of myocardial ischaemia and absence of significant CAD by invasive coronary angiography were scanned with static rest and stress CT perfusion. Myocardial attenuation densities were assessed at rest and during adenosine stress, segmented into 3 myocardial layers and 13 segments. MPR was higher in the subepicardium compared with the subendocardium (124% interquartile range [45, 235] vs. 68% [22,102], $P < 0.001$). Moreover, MPR in the septum was lower than in the inferolateral and anterolateral segments of the myocardium (55% [19, 104] vs. 89% [37, 168] and 124% [54, 270], $P < 0.001$). By multivariate analysis, high body mass index was significantly associated with reduced MPR in all myocardial layers when adjusted for cardiovascular risk factors ($P = 0.02$).

Conclusion In symptomatic patients without significant coronary artery stenosis, distinct differences in endocardial–epicardial distribution of perfusion reserve may be demonstrated with static CT perfusion. Low MPR in all myocardial layers was observed specifically in obese patients.

Keywords myocardial perfusion • multi-detector computed tomography • coronary artery disease

Introduction

Based on experimental animal studies, it is well established that the subendocardium is the part of the myocardium, which is most vulnerable to hypoperfusion and ischaemia.[1,2] In patients with suspected coronary artery disease (CAD), but without significant coronary artery stenosis by invasive coronary angiography (ICA), myocardial perfusion, and myocardial perfusion reserve (MPR) have been extensively studied.[3] These patients form a distinct and challenging clinical entity, in which coronary microvascular

* Corresponding author. Tel: +45 21 92 48 84; Fax: +45 35 45 28 75. E-mail: tobiaskh@gmail.com

dysfunction, in part, is thought to be responsible for symptoms and adverse prognosis.[4] Many studies have suggested an association between myocardial microvascular dysfunction and traditional cardiovascular risk factors, yet before the development of epicardial coronary stenosis and have furthermore suggested MPR as an important predictor of adverse outcomes.[5,6]

Previous patient studies have primarily assessed transmural myocardial perfusion and global left ventricular (LV) MPR. However, animal experimental studies have demonstrated large differences in MPR between the subepicardium and the subendocardium.[2] Consequently, important aspects of the transmural differences of myocardial perfusion and MPR from the endocardium to the epicardium in humans remain largely unknown.

Results from the CORE320 study have demonstrated that multidetector computed tomography (CT) myocardial perfusion (CTP) with adenosine stress is comparable with single-photon emission computed tomography (SPECT) myocardial perfusion imaging for the detection of perfusion abnormalities in patients with CAD.[7] In smaller patient populations with various presentations of CAD it has previously been demonstrated that transmural myocardial differences of perfusion may be assessed using CT with sub-millimetre spatial resolution.[8,9]

We sought to test the hypothesis that the MPR in all myocardial layers is determined by age, gender, and risk profile in patients with ischaemic symptoms or equivalent but with non-obstructive CAD by ICA.

Methods

Patient population and study design

Patients were included in the multicentre CORE320 trial (www.clinicaltrials.gov, NCT00934037) according to previously reported inclusion and exclusion criteria.[10] In brief, patients between 45 and 85 years of age with suspected or known CAD who were clinically referred for ICA were included in the trial. Clinical referral was due to chest pain or other symptoms suggestive of CAD including heart failure symptoms in combination with an abnormal ECG or stress test. Reasons for study exclusion were among others: known allergy to iodinated contrast media, elevated serum creatinine (1.5 mg/dL) or calculated creatinine clearance below 60 mL/min, atrial fibrillation, or evidence of acute coronary syndrome. Angina symptoms were recorded according to the Diamond and Forrester characteristics: substernal chest pain/discomfort, provoked by exertion or emotional distress, and relieved by rest and/or nitroglycerin. Typical angina was present if all characteristics were found. The research protocol, including SPECT, CTP, and clinically indicated ICA, was approved by the ethical committee of each participating centre, and all patients gave informed consent. For this CORE320 substudy, only patients without significant CAD by ICA were included. Patients were scanned with CT at rest and during adenosine stress, and based on myocardial attenuation values MPR was regionally assessed. The association between MPR and its possible determinants—predefined as age, gender, body mass index, race, diabetes, hypertension and dyslipidaemia, Agatston score, and abnormal SPECT—was assessed.

ICA and SPECT data acquisition and analysis

Clinically indicated ICA was performed within 60 days after CT examination. Coronary lesion severity was determined by quantitative coronary angiography according to standard methods. Patients were grouped according to ICA plaque severity, using quantitative coronary angiography as 'no or mild plaque' defined as a stenosis of 0–29% and 'moderate plaque' as 30–49%. Any lesion ≥50% was considered obstructive and such patients were excluded from this sub-study. SPECT acquisitions used ^{99m}Tc-labelled imaging agents, with ∼8 mCi for rest and 25 mCi for stress MPI studies. Stress testing with exercise or pharmacological stress agents (adenosine or dipyridamole) followed standard protocols and were performed in CORE320 qualified labs. Abnormal SPECT was defined as a single myocardial segment with a visually confirmed perfusion deficit at stress thought not to be secondary to artefact.

CT acquisition

The CT acquisition protocol of the CORE 320 study has previously been described in detail.[10] Before the CT angiography (CTA) examination patients with a heart rate >60 received oral (75–150 mg) or IV (up to 15 mg) metoprolol. Patients with systolic blood pressure 110 mmHg or higher received sublingual fast-acting nitrates, prior to CTA acquisition. The CTA and CTP acquisitions were performed with 50–70 mL of iodinated contrast according to body weight (Iopamidol 370 mg iodine/mL). The flow rate was 4–5 mL/s and was adjusted according to patient weight, as previously described in detail.[10] Prospective ECG-triggered image acquisition was performed using a peak tube voltage of 120 kV, a tube current of 300–550 mA according to body weight and a gantry rotation time of 0.350–0.375 s. Image acquisition was initiated by real-time bolus tracking with a target threshold of 300 HU in the descending aorta.

Twenty minutes after the rest examination with intravenous adenosine (0.14 mg/kg/min) was initiated and the stress CTP scan was performed after ∼4 min. Prospective ECG-triggered image acquisition was performed over one or two heart beats, depending on heart rate, using a peak tube voltage of 120 kV, a tube current of 270–470 mA according to body weight and a gantry rotation time of 0.350–0.375 s. Image acquisition was initiated by real-time bolus tracking with a target threshold of 300 HU in the descending aorta.

Real-time bolus tracking was performed for both the rest and stress scans, using a single 2 mm slice at the level of descending aorta and mid-left ventricle prior to and during contrast arrival. The real-time bolus tracking images prior to contrast arrival were used for myocardial baseline attenuation measurements.

Bolus tracking images and the rest and stress volumetric CTP images were reconstructed, using a myocardial perfusion kernel (FC03) without edge enhancement using filtered back projection and a beam-hardening correction algorithm described previously.[11] The R–R interval covered by prospective acquisition during CTP was between 75 and 95%. Rest and stress images were reconstructed at 1% intervals of the R–R cycle with 0.5 mm slice thickness, and the phase with least cardiac motion was selected for myocardial perfusion analysis.

CT image analysis

The primary outcome measure was global LV MPR defined as the percentage increase in baseline-corrected attenuation density (AD) between the rest and the stress (AD_{rest} and AD_{stress}) scan using the rest scan as reference: $MPR = (AD_{Stress} - AD_{Rest})/AD_{Rest.}$ For both rest and stress images, the mean attenuation density for rest and stress were assessed for each myocardial layer and for all myocardial segments. Baseline correction of the rest and stress myocardial attenuation densities was determined from the bolus tracking images prior to contrast arrival in the left ventricle. Baseline myocardial attenuation ($AD_{Baseline}$) was the mean attenuation measured across the three images. The

baseline-corrected AD for the rest and stress images were calculated as $AD_{Rest} - AD_{Baseline}$ and $AD_{Stress} - AD_{Baseline}$, respectively.

Values of AD were obtained using a commercially available software package (Myocardial Perfusion, Toshiba Medical Systems). An automatic border detection algorithm defined the endocardial and epicardial borders, and careful manual correction was done to avoid any inclusion of the left or right ventricular blood pool or any extra-cardiac tissue. An automated segmentation of the myocardium was done using a previously described 13 segment model, and the software provided the average AD values per myocardial segment.[12] Septum was defined as segments 2, 3, 8, 9, anterolateral segments were defined as segments 1, 6, 7, 12, and inferolateral segments as segments 4, 5, 10, 11. The apex, segment 13, was excluded from the analysis. The myocardium was automatically divided into three equally thick layers: the subendocardial, midmyocardial, and subepicardial layers (*Figure 1*).

Visual assessment of all myocardial segments was performed by two independent readers that noted any artefact from motion, beam-hardening, or cone beam as previously described.[13] Segments with artefacts were excluded from the analysis. LV mass was assessed from CT images.

Statistical analysis

All data were analysed in the statistical core laboratory at the Bloomberg School of Public Health. Myocardial attenuation density values are presented as median and interquartile range. Global and regional MPR in the LV septum, anterolateral and inferolateral myocardium were compared using pairwise Wilcoxon rank-sum tests. To test the primary hypothesis, first univariable analysis (linear regression or Wilcoxon rank-sum tests) was performed to evaluate determinants

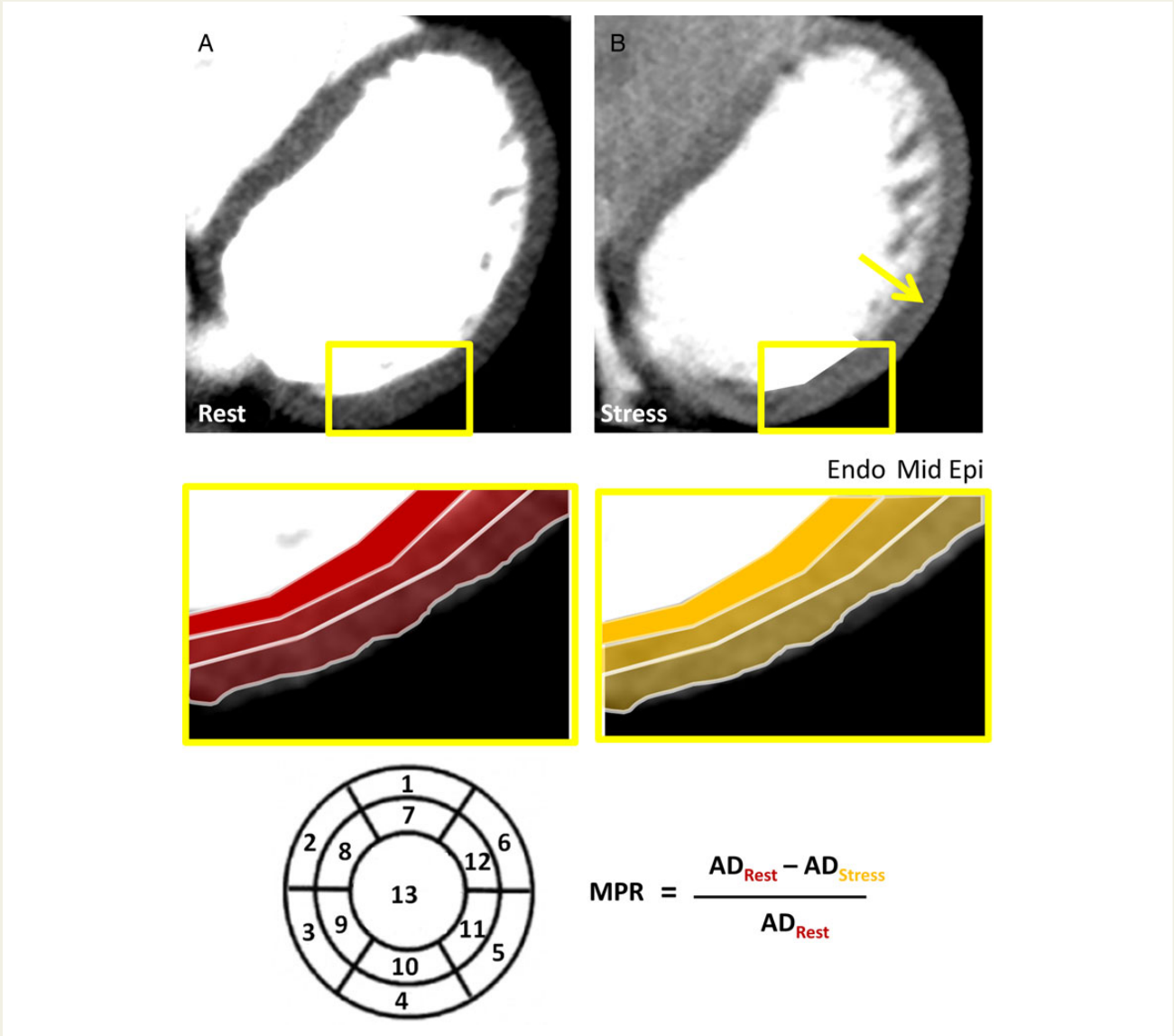

Figure 1 Attenuation density (AD) was measured in 3 myocardial layers (endo-, mid-, and epi-) and 13 segments during rest (*A*: AD_{Rest}) and during adenosine stress (*B*: AD_{Stres}). From these measurements regional and global MPR was calculated using the given formula. A difference in endo- to epi-perfusion reserve is noted during adenosine with markedly higher perfusion in the epi layer (*B*: yellow arrow).

(body mass index, coronary calcium, ICA plaque severity, gender, race, diabetes, hypertension, dyslipidaemia, and LV mass) of MPR (outcome). Upon identification of body mass index as a determinant of MPR, a series of nested multivariable linear regression models were performed. The base models included age, body mass index, coronary calcium, gender, race, diabetes, hypertension, dyslipidaemia, and abnormal SPECT result as predictors; the second model was nested in the first and included LV mass. The threshold of significance was $P < 0.05$. Statistical analyses were performed using SAS 9.2, Stata 11, and SPlus 8.0.

Results

A total of 381 patients were included in the CORE320 study, and out of these patients 149 (39%) were free of obstructive CAD by ICA. Patient demographics are presented in *Table 1*. Mean heart rate during rest was 55 [50–59] bpm increasing to 72 [65–80] during adenosine stress ($P < 0.001$). The proportion of patients with no coronary disease (no plaque) on ICA was 8. The proportion of patients with a mild quantitative coronary angiography stenosis of 1–29% was 86/149, 58% and the proportion of patients with moderate stenosis (30–49%) was 55/149, 37%.

Patients received a median radiation dose of 3.2 mSv (IQR: 2.8–3.5) for CTA and 5.2 (3.9–6.0) mSv for CTP.

Myocardial perfusion and perfusion reserve

LV myocardial attenuation density values for rest and stress are presented in *Table 2*. In the whole study group, the median, baseline-corrected transmural myocardial AD was 24 [19, 31] HU at rest and 43 [33–52] HU at stress ($P < 0.001$) resulting in an overall median transmural MPR of 104% [37–172%]. We found an increasing median MPR in the endo- to epi-direction with a significantly lower median MPR in the subendocardial myocardium compared with mid- and subepicardial layers (*Figure 2*).

Global LV (top) and regional transmural differences of MPR between LV walls (bottom) are given in *Figure 3*. The MPR in the septum was 2.3 and 1.6 times lower compared with anterolateral and inferolateral regions. The lower MPR in the septum was caused by a higher rest attenuation in the septum compared with anterolateral and inferolateral segments (33 vs. 15 HU and 22 HU, $P < 0.0001$ for both), which was more pronounced in the epicardial layer (32 vs. 9 HU and 14 HU) compared with the endocardial layer (37 vs. 24 HU and 29 HU).

Determinants of MPR

Univariate correlations to MPR are presented in *Table 3*. There was no difference in AD_{rest}, AD_{stress}, and MPR between patients with and without abnormal SPECT, as presented in *Figure 4*. In men but not in women, MPR was found to be inversely correlated to age ($MPR_{transmural}$, $P = 0.04$). There was a tendency towards lower MPR in patients with diabetes and hypertension, but this was not significant. A significant inverse correlation between MPR_{endo} and LV mass was noted (estimate -0.002, $P = 0.03$).

We found patients with non-significant moderate coronary plaque as determined by ICA to have a median global MPR of 107 (IQR 39–184) compared with 103 (IQR 37–165, $P =$ NS) in patients with no or mild plaque.

Table 1 Demographic characteristics

Characteristic	*N* (%) or Median [IQR]
Number of patients	149
Age, years	61 [54, 67]
Male sex	75 (50.3)
Race (African-American)	21 (14.1)
Height	165 [158, 172]
BMI	27.3 [24.4, 31.2]
<25 (normal weight)	44 (29.5%)
25–30 (overweight)	54 (36.2%)
>30 (obese)	51 (34.2%)
Hypertension	106 (71.6)
Diabetes	43 (28.9)
Current smoker	29 (20.0)
Family history of CAD	61 (42.4)
Previous myocardial infarction	20 (13.4)
Dyslipidaemia	82 (56.2)
Coronary calcium score	
Overall	9 [0, 118]
Agatston score 0	53 (35.6%)
Agatston score 1–10	22 (14.8%)
Agatston score 11–100	34 (22.8%)
Agatston score 101–400	28 (18.8%)
Agatston score >400	12 (8.1%)
Angina at presentation	
Typical	37 (25%)
Atypical	77 (52%)
Other signs/symptoms suggestive of CAD[a]	35 (23%)
Medication (per cent of patients)	
Nitro	19 (12.8)
Beta blocker	73 (49.0)
Calcium channel blocker	27 (18.1)
ACE/ARB	74 (49.7)
Other antihypertensive medication	35 (23.5)
Patients with positive SPECT	50 (33.6)

ACE, angiotensin-converting enzyme inhibitors; ARB, angiotensin receptor blockers; BMI, body mass index; IQR, interquartile range; SPECT, single-photon emission computed tomography; CAD, coronary artery disease.
[a]Other signs/symptoms suggestive of CAD: heart failure symptoms, shortness of breath, abnormal ECG or stress test.

By univariate analysis we found that transmural MPR was significantly determined by body mass index; comparisons between BMI groups for AD_{rest}, AD_{stress}, and MPR are presented in *Figure 5*. Lower MPR in obese patients appears to be the consequence of higher baseline perfusion values. In women a slightly higher median AD_{rest} (25 vs. 21 HU, $P = 0.002$) and moderately higher AD_{stress} compared with men (49 vs. 34 HU, $P < 0.0001$) was noted. This pattern was found in all myocardial layers; however, there was no significant difference between genders for MPR women vs. men (Transmural MPR: 108% vs. 99%, $P = 0.34$).

Multivariate analysis showed that BMI is inversely correlated with MPR both transmural (see *Table 3*), subendocardial ($\alpha = -0.03$,

Table 2 Attenuation density values of rest and stress in all myocardial layers

	Rest		Stress	
	Median [IQR]	Mean ± SD	Median [IQR]	Mean ± SD
Attenuation density un-corrected				
Transmural	73.7 [67.2, 79.2]	73.8 ± 10.5	103.8 [93.7, 112.5]	103.9 ± 13.5
Endo-layer	79.0 [74.3, 86.9]	80.9 ± 11.1	109.3 [99.5, 118.1]	109.8 ± 14.2
Mid-layer	72.9 [67.0, 79.1]	73.8 ± 10.5	105.8 [95.5, 114.2]	105.6 ± 13.9
Epi-layer	66.0 [59.7, 70.8]	65.9 ± 9.6	95.5 [86.0, 104.3]	95.6 ± 12.6
Attenuation density baseline-corrected				
Transmural	24.0 [18.9, 31.2]	26.0 ± 12.2	42.9 [32.6, 51.7]	42.9 ± 14.5
Endo-layer	30.6 [24.7, 37.7]	32.7 ± 13.1	48.1 [38.2, 58.0]	48.7 ± 15.3
Mid-layer	24.3 [18.9, 31.2]	26.5 ± 12.2	44.6 [34.3, 54.4]	44.9 ± 14.9
Epi-layer	18.7 [14.9, 24.2]	20.7 ± 10.1	35.9 [26.4, 45.9]	36.2 ± 12.8

SD, standard deviation; IQR, interquartile range.

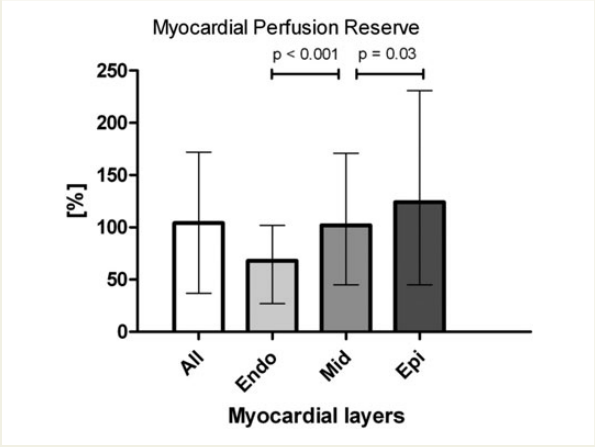

Figure 2 Bar diagram of the difference in MPR between the myocardial layers. Results presented in median and interquartile range.

$P = 0.002$), and mid-myocardial ($\alpha = -0.06$, $P = 0.004$), however, not subepicardial ($\alpha = -0.05$, $P = 0.07$). In the multivariate analysis, gender was not associated with transmural MPR, however, in the subendocardial layer, a higher MPR was associated with female gender ($P = 0.02$). Adding LV mass to the abovementioned model did not change the results. Replacing CACS with ICA assessment of plaque severity in the model did also not change the results.

The effect of BMI on MPR was maintained in patients with angina symptoms, with the strongest signal in the endo- and mid-layer (MPR_{endo} $P = 0.002$, MPR_{mid} $P = 0.002$, MPR_{epi} $P = 0.05$, $MPR_{transmural}$ $P = 0.005$, adjusted model), whereas no effect was found in patients without chest pain symptoms.

Discussion

In the current study, we have demonstrated that symptomatic patients with a variable number of cardiovascular risk factors and absence of coronary artery stenosis display significant differences in endocardial–epicardial distribution of myocardial perfusion and perfusion reserve. Low MPR in both endocardial, mid-, and subendocardial layers was observed specifically in obese patients. The endocardial–epicardial distribution of increasing MPR in the endo- to epi-direction observed in these patients appears to correlate with similar perfusion patterns reported in animal models.[14]

Our results appear to be in concordance with previous studies that have reported an association between obesity and impaired endothelial dysfunction in both peripheral and coronary circulation.[6,15,16] In contrast to previous studies, we found that reduced MPR as assessed by CT in obese patients was the result of an increase in AD_{rest} values rather than reduced vasodilator response to adenosine. The explanation for this difference compared with previous studies remains unknown, but could be related to differences of patient selection and/or methodology used. It is noteworthy that differences of resting perfusion between normal and obese in our study were unrelated to age and gender in the groups that could suggest that increased body weight was the determining factor for our finding.

We found the effect of BMI on MPR was only observed in patients with chest pain symptoms and not in patients without. However as the subgroup of patients without chest pain symptoms was small, this finding could be due to low statistical power.

Previous studies have shown that women have a higher coronary bloodflow at rest compared with men, which is confirmed in our study.[17–19] Chareonthaitawee *et al.* found that this resulted in an overall lower MPR in women. However, in accordance with other studies we did not find a significant difference in MPR between women and men.[18,19]

Age has previously been inversely associated with MPR by Czernin *et al.*, studying an asymptomatic healthy population with a broad age span [19–86 year].[20] Despite a lower age span in our study (interquartile range 54–67 years), we were able to reproduce this inverse correlation in men.

We had expected diabetes and hypertension to have significant impact on MPR as this has previously been reported in studies using

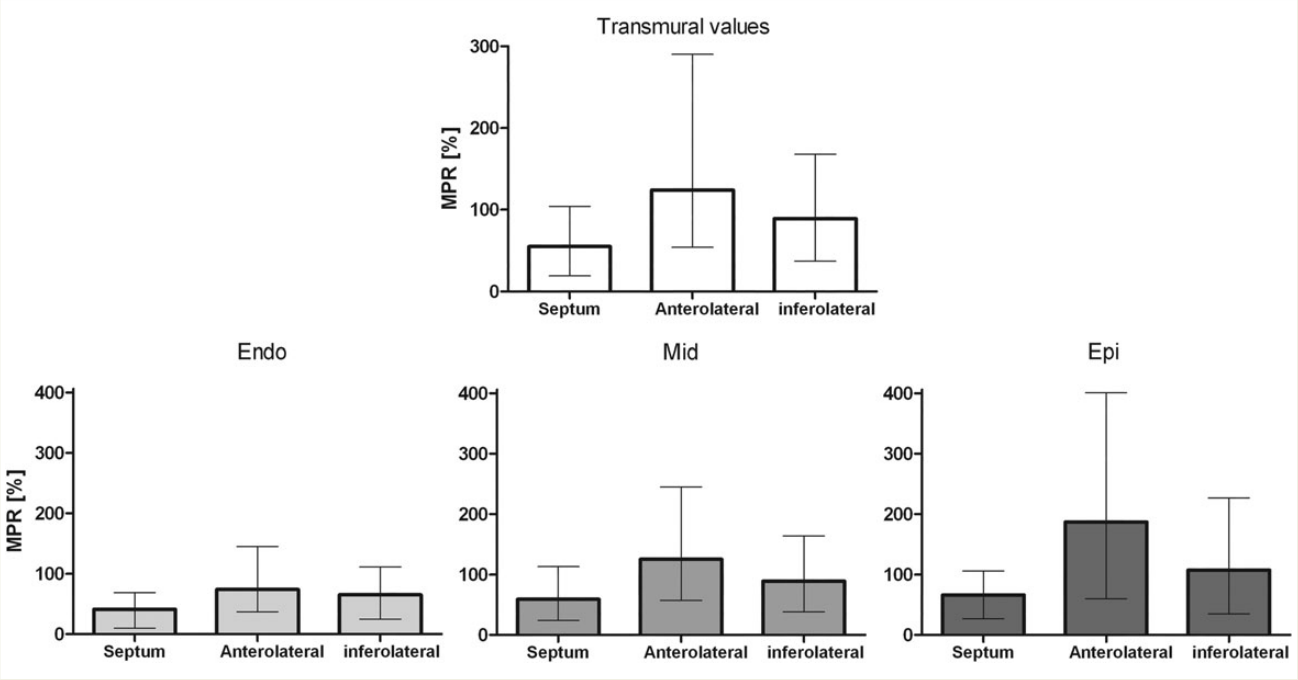

Figure 3 Regional MPR in the LV septum, anterolateral, and inferolateral myocardium. For transmural myocardial values and each myocardial layer. Septum vs. anterolateral, septum vs. inferolateral, and anterolateral vs. inferolateral were all significantly different ($P < 0.05$).

positron emission tomography (PET) and cardiac magnetic resonance imaging, but did only find a trend.[21] This could be explained by a lower sensitivity of the static CT perfusion method compared with dynamic PET. Nevertheless, we demonstrated an inverse correlation between subendocardial MPR and LV mass, the latter which to some extent reflects extent of organ damage related to hypertension and/or diabetes—in accordance with earlier PET reports.[22]

We observed a pattern of higher endocardial than epicardial blood flow during both rest and stress, and moreover that adenosine MPR increases in the endocardial to epicardial direction. Cardiac contraction impedes myocardial blood flow. During systole, the myocardial compressive force increases from intrathoracic pressure at the epicardial surface to equal or to exceed intraventricular pressure at the endocardial surface.[23] The limited systolic flow is directed towards the epicardium and blood in the deepest subendocardial layers is squeezed retrograde into more superficial subepicardial arterial vessels. Despite these mechanical effects that increase impedance to blood flow in the deeper myocardial layers, it is a consistent finding across more than 20 animal studies using microsphere derived blood flow that there is a net transmural gradient of blood favouring the subendocardium, which reflect oxygen requirements of the subendocardium.[24] This requires an augmentation of subendocardial blood flow during diastole in proportion to the degree of systolic underperfusion. This diastolic gradient of blood flow favouring the subendocardium is dependent on a transmural gradient of vasomotor tone, with vascular resistance during diastole being lowest in the subendocardium.[14] Relative myocardial perfusion as assessed with CT is a measure of diastolic flow distribution and especially in this phase of the cardiac cycle (and during rest) the gradient of vasomotor tone appears to be a major determinant of the preferential subendocardial blood flow supply.[14] The uncoupling of regional energetic demands and myocardial flow by pharmacological vasodilation with adenosine—that acts by relaxation of vascular smooth muscle cells of resistance vessels—appears to result in a partly offsetting of the transmural differences of vasomotor tone resulting in a higher epicardial flow reserve. In concordance with a previous magnetic resonance imaging study, our observations confirm that in symptomatic patients—without obstructive CAD—there is a significant adenosine-induced increase in both subendocardial and subepicardial perfusion and moreover that subepicardial MPR is higher than subendocardial.[25] Thus, we found no evidence of subendocardial ischaemia in these patients.

We found that the transmural MPR in the septum was 2.3 and 1.6 times lower compared with that of anterolateral and inferolateral regions of the myocardium. This is in concordance with a recent magnetic resonance study in healthy subjects, which found a septal MPR that was 1.4–1.6 times lower than the rest of the myocardium.[26] Our study suggests that the higher septal MPR is due to higher resting flow in the septum. This was most pronounced in the septal subepicardium that faces right ventricular systolic pressure and therefore in terms of regional pressure conditions is more equated with subendocardium.

There was no detectable difference in MPR between patients with and without one or more abnormal myocardial segments by SPECT. This could partly be explained by regional myocardial differences with compensatory regional hyperperfusion in SPECT normal segments. Also the presence of false-positive SPECT and the sensitivity of the methods used could have influenced the results

Table 3 Determinants of MPR in univariable and multivariable analysis

Variable	Univariable analysis		Multivariable regression analysis	
	Median [IQR]	*P*-value	Estimate	*P*-value
Binary				
Male gender				
No	107 [54–165]	0.31	−0.25	0.22
Yes	99 [31–181]			
Black race				
No	101 [34–165]	0.70	0.23	0.42
Yes	110 [30–207]			
Diabetes				
No	110 [49–183]	0.12	−0.09	0.67
Yes	75 [14–152]			
Hypertension				
No	113 [54–192]	0.28	−0.20	0.41
Yes	96 [32–170]			
Dyslipidaemia				
No	103 [37–157]	0.56	0.24	0.25
Yes	106 [44–185]			
Abnormal SPECT				
No	103 [34–161]	0.83	0.01	0.97
Yes	102 [44–181]			
Continuous	**Estimate**	***P*-value**		
Age	−0.01	0.48	−0.01	0.37
Body mass index	−0.04	0.039	−0.05	0.02
Coronary artery calcium score	0.0001	0.42	0.0003	0.21

SPECT, single-photon emission computed tomography.

Limitations

We describe flow patterns in patients suspected of CAD, but without coronary artery stenosis as verified by ICA. In the future, it will be important to further decrease radiation dose associated with CTP to permit the assessment of reference values in healthy individuals.

No reference method was used to substantiate the CT findings with regard to physiological transmural flow distribution in humans. Yet, CT has been well validated in animal experimental models[27] and although MR and PET may provide some information with regard to differences in the transmural perfusion distribution they are limited by lower spatial resolution compared with CT.

We used a beam hardening correction algorithm that has been validated using myocardial phantoms and animal models of coronary ischaemia and found that beam-hardening artefacts can be adequately corrected for.[11] All cardiac segments were carefully analysed and excluded from further analysis at the presence of artefacts. Nevertheless we cannot exclude that image motion or other artefacts may have affected attenuation values to some extent.

The present study uses adenosine as stressor, thus we are measuring both endothelium-dependent and non-endothelium-dependent flow changes. A true reflection of endothelium-dependent microvascular function would be a response to acetylcholine or a cold pressor test.

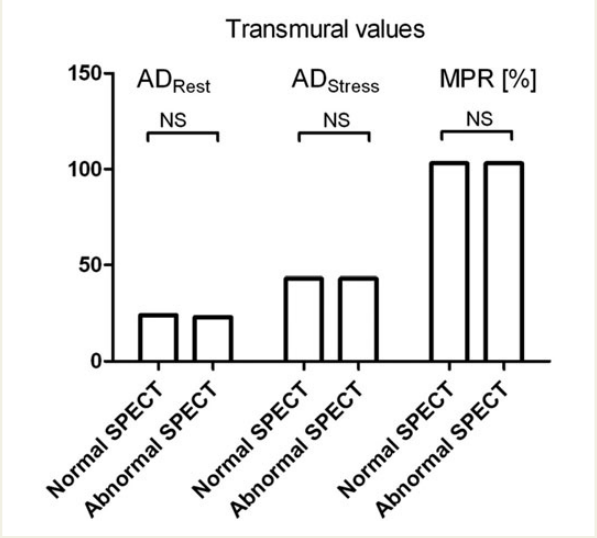

Figure 4 Differences between patients with and without abnormal SPECT, showing median values of myocardial attenuation at rest (AD_{Rest}) and during pharmacological vasodilation (AD_{Stress}) and MPR (in %).

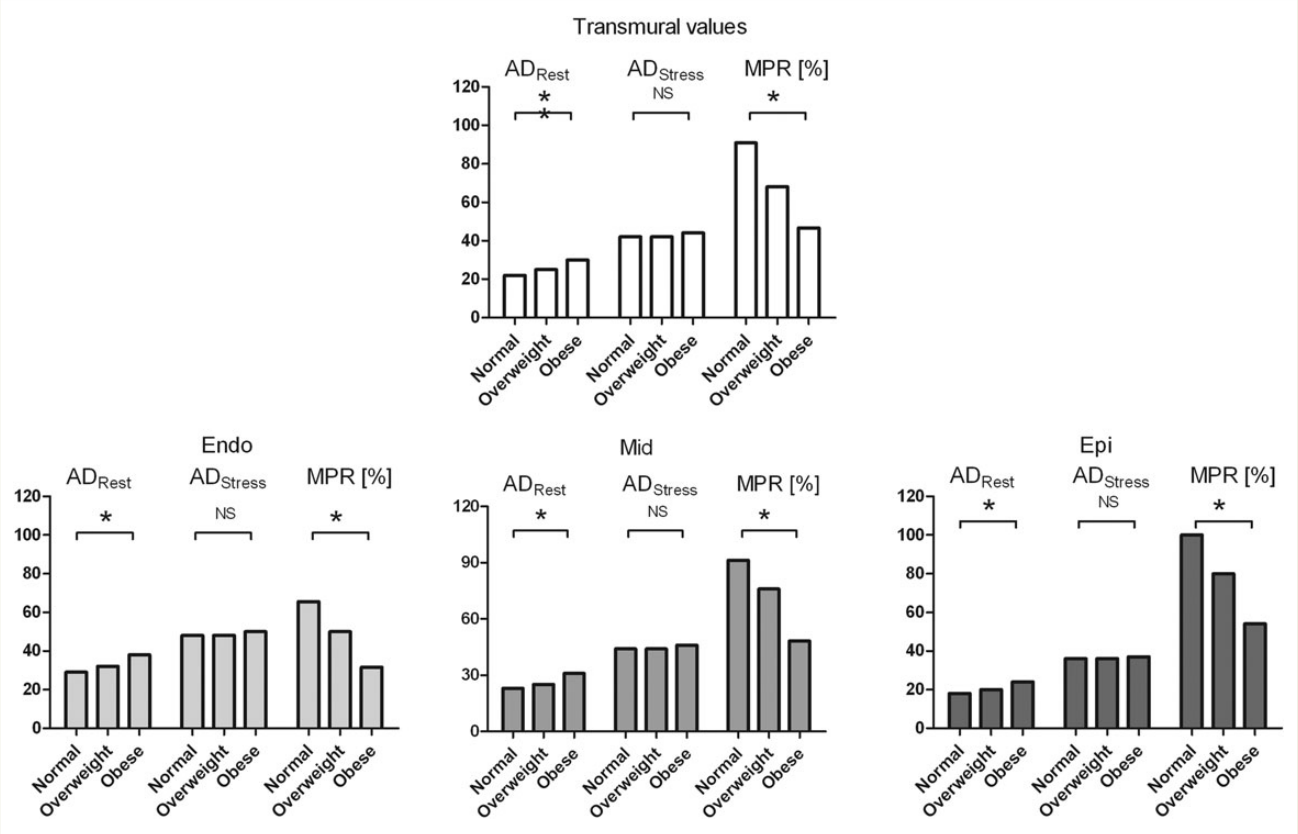

Figure 5 Differences between body mass index groups for median values of myocardial attenuation at rest (AD_{Rest}) and during pharmacological vasodilation (AD_{Stress}) in baseline-corrected Hounsfield Unit values. Differences between BMI groups for median MPRare in %. *$P \leq 0.01$ between normal weight and obesity.

Interobserver variability of MPR measurements was not assessed. However, using the same method for assessment of segmental AD_{rest} and AD_{Stress} we previously found a mean difference of 2 ± 1 HU with 95% limits of agreement from 0 to 3 HU.[9]

Our study uses a static CT perfusion image that only provides the relative difference between rest and stress. In contrast dynamical CT perfusion imaging is a promising technique that may provide reliable measures absolute myocardial bloodflow during both rest and hyperaemia, which could provide a more accurate assessment than static CT.[28]

Conclusion

In patients with suspicion of CAD, but free of significant coronary artery stenosis, the MPR increases in the endocardial to epicardial direction. The epicardial perfusion reserve was reduced in the ventricular septum, contributing to an overall transmural reduced MPR in this region. High body weight was the strongest independent determinant of MPR in all layers of the myocardium.

Acknowledgements

The authors wish to thank Andrea Vavere for invaluable help and Chris Cox for the statistical work.

Conflict of interest: K.F.K., M.D.C., R.T.G., M.D., K.K., V.C.M., and J.A.C.L. report institutions receive grant support from Toshiba Medical System. K.F.K., M.D.C., K.F.K., and J.A.C.L. report institution or individual receives support for travel to meetings for the study or other purposes from Toshiba Medical Systems. K.F.K., J.J.L., M.D., and J.T.K. have received lecture fees from Toshiba Medical Systems. M.D. has received lecture fees from Guerbet, Cardiac MR Academy Berlin, and Bayer (Schering-Berlex). M.D. has received grant support from GE Healthcare, Bracco, Guerbet, and Toshiba Medical Systems. K.K. reports grant support from GE Healthcare, Philips Electronics, Bayer, Gerber, and Eisai. R.T.G. reports institution receives grant support from GE Healthcare and consultancy for ICON Medical Imaging. J.A.C.L. receives grant support from Bracco Diagnostics. K.F.K. receives grants from the Danish Heart Foundation, The John and Birte Meyer Foundation, and the A. P. Moller and Chastine Mc-Kinney Møller Foundation. J.T.K. is supported by The Research Fund of Rigshospitalet, Copenhagen University Hospital.

Funding

The study sponsor, Toshiba Medical Systems Corporation, was not involved in any stage of the study design, data acquisition, data analysis, or manuscript preparation.

References

1. Reimer KA, Lowe JE, Rasmussen MM, Jennings RB. The wavefront phenomenon of ischemic cell death. 1. Myocardial infarct size vs. duration of coronary occlusion in dogs. *Circulation* 1977;**56**:786–94.
2. Duncker DJ, Bache RJ. Regulation of coronary blood flow during exercise. *Physiol Rev* 2008;**88**:1009–86.
3. Schindler TH, Schelbert HR, Quercioli A, Dilsizian V. Cardiac PET imaging for the detection and monitoring of coronary artery disease and microvascular health. *JACC Cardiovasc Imaging* 2010;**3**:623–40.
4. Crea F, Camici PG, Bairey Merz CN. Coronary microvascular dysfunction: an update. *Eur Heart J* 2014;**35**:1101–11.
5. Schindler TH, Nitzsche EU, Schelbert HR, Olschewski M, Sayre J, Mix M *et al.* Positron emission tomography-measured abnormal responses of myocardial blood flow to sympathetic stimulation are associated with the risk of developing cardiovascular events. *J Am Coll Cardiol* 2005;**45**:1505–12.
6. Schindler TH, Cardenas J, Prior JO, Facta AD, Kreissl MC, Zhang XL *et al.* Relationship between increasing body weight, insulin resistance, inflammation, adipocytokine leptin, and coronary circulatory function. *J Am Coll Cardiol* 2006;**47**:1188–95.
7. Rochitte CE, George RT, Chen MY, Arbab-Zadeh A, Dewey M, Miller JM *et al.* Computed tomography angiography and perfusion to assess coronary artery stenosis causing perfusion defects by single photon emission computed tomography: the CORE320 study. *Eur Heart J* 2014;**35**:1120–30.
8. George RT, Arbab-Zadeh A, Miller JM, Kitagawa K, Chang HJ, Bluemke DA *et al.* Adenosine stress 64- and 256-row detector computed tomography angiography and perfusion imaging: a pilot study evaluating the transmural extent of perfusion abnormalities to predict atherosclerosis causing myocardial ischemia. *Circ Cardiovasc Imaging* 2009;**2**:174–82.
9. Kuhl JT, Linde JJ, Fuchs A, Kristensen TS, Kelbaek H, George RT *et al.* Patterns of myocardial perfusion in humans evaluated with contrast-enhanced 320 multidetector computed tomography. *Int J Cardiovasc Imaging* 2012;**28**:1739–47.
10. George RT, Arbab-Zadeh A, Cerci RJ, Vavere AL, Kitagawa K, Dewey M *et al.* Diagnostic performance of combined noninvasive coronary angiography and myocardial perfusion imaging using 320-MDCT: the CT angiography and perfusion methods of the CORE320 multicenter multinational diagnostic study. *AJR Am J Roentgenol* 2011;**197**:829–37.
11. Kitagawa K, George RT, rbab-Zadeh A, Lima JA, Lardo AC. Characterization and correction of beam-hardening artifacts during dynamic volume CT assessment of myocardial perfusion. *Radiology* 2010;**256**:111–8.
12. Cerci RJ, Arbab-Zadeh A, George RT, Miller JM, Vavere AL, Mehra V *et al.* Aligning coronary anatomy and myocardial perfusion territories: an algorithm for the CORE320 multicenter study. *Circ Cardiovasc Imaging* 2012;**5**:587–95.
13. Mehra VC, Valdiviezo C, Arbab-Zadeh A, Ko BS, Seneviratne SK, Cerci R *et al.* A stepwise approach to the visual interpretation of CT-based myocardial perfusion. *J Cardiovasc Comput Tomogr* 2011;**5**:357–69.
14. Bache RJ, Cobb FR. Effect of maximal coronary vasodilation on transmural myocardial perfusion during tachycardia in the awake dog. *Circ Res* 1977;**41**:648–53.
15. Al SJ, Higano ST, Holmes DR Jr, Lennon R, Lerman A. Obesity is independently associated with coronary endothelial dysfunction in patients with normal or mildly diseased coronary arteries. *J Am Coll Cardiol* 2001;**37**:1523–8.
16. Steinberg HO, Chaker H, Leaming R, Johnson A, Brechtel G, Baron AD. Obesity/insulin resistance is associated with endothelial dysfunction. Implications for the syndrome of insulin resistance. *J Clin Invest* 1996;**97**:2601–10.
17. Byrne C, Kühl JT, Zacho M, Nordestgaard BG, Fuchs A, Frestad D *et al.* Sex- and age-related differences of myocardial perfusion at rest assessed with multidetector computed tomography. *J Cardiovasc Comput Tomogr* 2013;**7**:94–101.
18. Chareonthaitawee P, Kaufmann PA, Rimoldi O, Camici PG. Heterogeneity of resting and hyperemic myocardial blood flow in healthy humans. *Cardiovasc Res* 2001;**50**:151–61.
19. Duvernoy CS, Meyer C, Seifert-Klauss V, Dayanikli F, Matsunari I, Rattenhuber J *et al.* Gender differences in myocardial blood flow dynamics: lipid profile and hemodynamic effects. *J Am Coll Cardiol* 1999;**33**:463–70.
20. Czernin J, Muller P, Chan S, Brunken RC, Porenta G, Krivokapich J *et al.* Influence of age and hemodynamics on myocardial blood flow and flow reserve. *Circulation* 1993;**88**:62–9.
21. Kawecka-Jaszcz K, Czarnecka D, Olszanecka A *et al.* Myocardial perfusion in hypertensive patients with normal coronary angiograms. *J Hypertens* 2008;**26**:1686–94.
22. Choudhury L, Rosen SD, Patel D, Nihoyannopoulos P, Camici PG. Coronary vasodilator reserve in primary and secondary left ventricular hypertrophy. A study with positron emission tomography. *Eur Heart J* 1997;**18**:108–16.
23. Archie JP Jr. Transmural distribution of intrinsic and transmitted left ventricular diastolic intramyocardial pressure in dogs. *Cardiovasc Res* 1978;**12**:255–62.
24. Westerhof N, Boer C, Lamberts RR, Sipkema P. Cross-talk between cardiac muscle and coronary vasculature. *Physiol Rev* 2006;**86**:1263–308.
25. Vermeltfoort IA, Bondarenko O, Raijmakers PG, Odekerken DA, Kuijper AF, Zwijnenburg A *et al.* Is subendocardial ischaemia present in patients with chest pain and normal coronary angiograms? A cardiovascular MR study. *Eur Heart J* 2007;**28**:1554–8.
26. Muehling OM, Jerosch-Herold M, Panse P, Zenovich A, Wilson BV, Wilson RF *et al.* Regional heterogeneity of myocardial perfusion in healthy human myocardium: assessment with magnetic resonance perfusion imaging. *J Cardiovasc Magn Reson* 2004;**6**:499–507.
27. George RT, Jerosch-Herold M, Silva C, Kitagawa K, Bluemke DA, Lima JA *et al.* Quantification of myocardial perfusion using dynamic 64-detector computed tomography. *Invest Radiol* 2007;**42**:815–22.
28. Ho KT, Ong HY, Tan G, Yong QW. Dynamic CT myocardial perfusion measurements of resting and hyperaemic blood flow in low-risk subjects with 128-slice dual-source CT. *Eur Heart J Cardiovasc Imaging* 2015;**16**:300–6.